



Performance Analysis of ACO-OFDM Visible Light Communication System Based on SCMA

Xiukai Ruan¹ and Shahid Iqbal Awan^{2,*}

¹Institute of Intelligent Lock, Wenzhou University, Wenzhou, China

²University of Poonch Rawalakot, Rawalakot, Pakistan

*Corresponding Author: Shahid Iqbal Awan. Email: ShahidAwan@jxyy.edu.cn

Received: 05 November 2022; Accepted: 06 December 2022; Published: 10 July 2023

Abstract: A SCMA ACO-OFDM downlink visible light communication (VLC) system is proposed. Six users share four spectrum resources, four of which are 4 primary color LED lights. ACO-OFDM technology is used to convert the user's sparse codebook mapped signal into a positive real value signal that can be carried on the light wave, which can realize high-speed parallel communication. Simulation verifies the feasibility of the system. At the same time, the channel model of visible light communication is constructed, and the signal-to-noise ratio(SNR) and channel gain of the visible light channel are systematically analyzed. Finally, the theoretical bit error rate formula using MPA decoding algorithm under different codebook constellation mapping points is given. Through simulation, it is verified that the theoretical bit error rate formula is basically consistent with the simulation bit error rate formula.

Keywords: SCMA; ACO-OFDM; visible light communication; SNR; MPA; bit error rate

1 Introduction

Visible light communication technology is increasingly favored by many researchers. It has the advantages of high-speed communication, low interference effect compared with traditional RF communication, high security and green environmental protection, and is expected to become the next-generation technology for mobile communication [1–3]. Similarly, Non-Orthogonal multiple access (NOMA) technology also has many advantages, such as being able to support a larger number of users to achieve high-quality communication under the same spectrum resources. Compared with orthogonal multiple access (OMA) technology, it is also expected to become the next generation mobile communication technology [4,5]. Therefore, it is very meaningful to consider the combination of visible light communication (VLC) technology and Non-Orthogonal multiple access (NOMA) technology. Its advantages are mainly reflected in the following points: 1. VLC users can realize high-quality communication in overloaded indoor scenes; 2. It can make the limited visible spectrum resources achieve greater communication capacity; 3. In the visible light communication scene with



This work is licensed under a Creative Commons Attribution 4.0 International License, which permits unrestricted use, distribution, and reproduction in any medium, provided the original work is properly cited.

high signal-to-noise ratio (SNR), Noam technology has better communication performance than OMA technology, such as higher bit error rate and higher utilization of low-frequency spectrum [4].

In order to realize high-speed visible light communication, researchers have proposed to apply OFDM technology to visible light communication, and OFDM technology has high frequency band utilization, strong anti-fading ability, strong resistance to inter-symbol interference as well as inter-symbol interference, and has the benefits of being suitable for high-speed data transmission. ACO-OFDM technology is a hot technology now, One of the biggest advantages of ACO-OFDM modulation is that in a typical visible light communication system, we can only use intensity modulation/direct detection (IM/DD), and the data is carried under the intensity of the optical signal, so it can only be a positive real value signal, while the baseband signal of OFDM is usually a complex bipolar signal. According to the principle of IFFT transformation, if the frequency domain vector before IFFT transformation meets Hermitical symmetry, we can get a real baseband signal. The single polarization of the obtained real baseband signal can meet the requirements of intensity modulation/direct detection (IM/DD). The earliest proposed method of single polarization OFDM is DCO-OFDM. In DCO-OFDM, the negative signal is eliminated by adding DC bias, and a positive real signal is obtained. However, because the large peak to average ratio of OFDM system will reduce the efficiency of the power amplifier of the transmission system, the DC bias cannot be too large, Moreover, even if the DC offset is large, some signals will still be negative, and further amplitude limiting is needed, which not only increases the transmission power, but also leads to signal distortion, which seriously affects the communication performance of the system. In order to avoid such limiting noise and nonlinear distortion, researchers also proposed ACO-OFDM technology. In ACO-OFDM system, unipolar signals are obtained by limiting the amplitude of bipolar signals. If only information is sent on odd carriers, all limiting noise will be on even carriers, and the information sent on odd carriers will not be affected, and the correct selection of carrier frequency at the receiving end, It can accurately restore the original sent information. The OFDM system using this technology is significantly better than on-off keying (OOK), pulse position modulation (PPM) and DCO-OFDM technology in terms of optical power efficiency, so here we also use ACO-OFDM technology [6].

Non orthogonal multiple access technology (NOMA) is a key technology of 5g communication system physical layer architecture [7]. Now there are two well-developed NOMA technologies, namely power domain non orthogonal multiple access (PD-NOMA) [8] and code domain non orthogonal multiple access, that is, sparse code multiple access (SCMA) [9]. NOMA technology puts forward a new theoretical dimension, that is, in the power domain, different users share the same spectrum resources, and the receiver uses serial interference cancellation (SIC) technology to eliminate the interference between different users. SCMA technology is a code domain non orthogonal multiple access technology proposed by Huawei. Compared with the previous low-density signature (LDS) technology, SCMA technology has the advantages of lower complexity and better communication performance [9,10]. In the SCMA communication system, the input bit information stream is mapped into multi-dimensional code words by the SCMA codebook, and the message passing (MPA) algorithm is used at the receiving end to eliminate the interference between users and decode the bit information of each user [11]. Among them, the design of sparse codebook plays an important decisive factor for the performance of SCMA system.

In previous studies, some researchers proposed a color domain SCMA non orthogonal multiple access visible light communication system, and analyzed the theoretical BER upper bound of the system [12]; Reference [13] proposed a visible light communication system combining PD-NOMA and SCMA; The literature proposes a visible light communication system based on SCMA, and compares

it with the bit error rate of OMA multiple access OFDMA technology [14,15]; The literature proposes BER analysis of SCMA system based on Star QAM signal constellation codebook design [16].

Some of the above studies only put forward a system concept, and did not analyze the performance of the system theoretically, such as theoretical error rate analysis. Some did error rate analysis, but the theoretical analysis was not accurate enough. In this paper, we not only make the downlink system model of ACO-OFDM visible light communication based on SCMA, but also analyze the channel model and noise of the system, and give a more accurate bit error rate formula. The simulation results show that our theoretical analysis and simulation results are consistent.

2 System Model

As shown in Fig. 1, assume a downlink multi-user SCMA visible light communication system, where users share resources. Here, we assume that six users share four resources, four of which represent four frequency points of four primary color LED lights. Here we use ACO-OFDM modulation technology. Next, we will discuss it in three parts: sender, channel model and receiver.

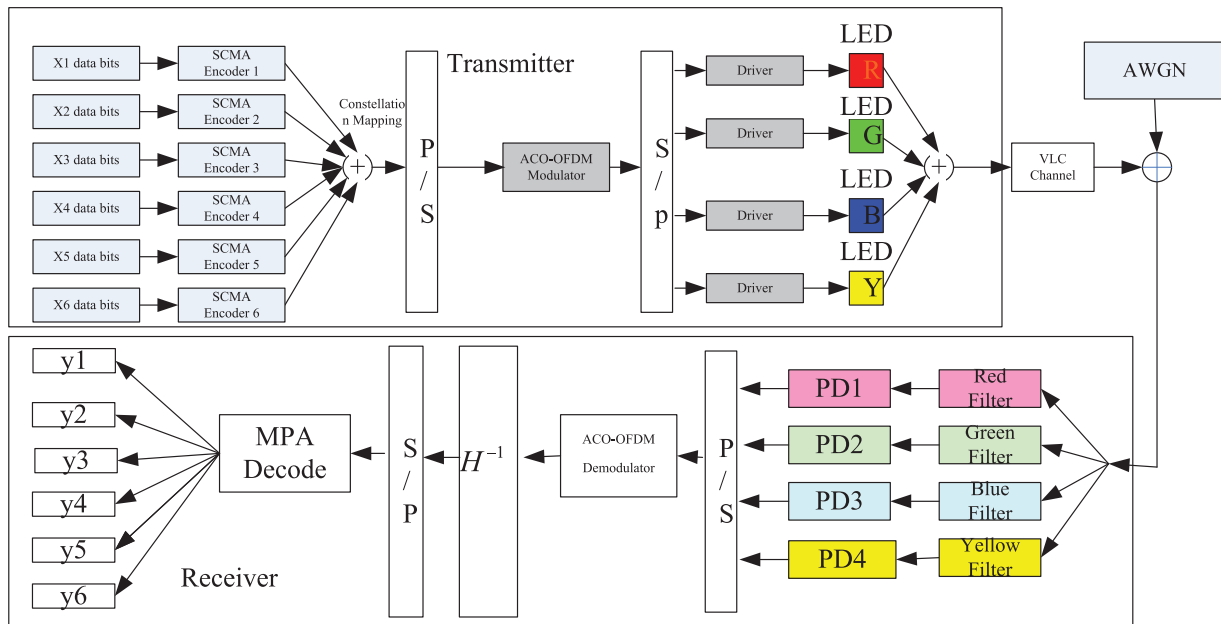


Figure 1: System model

2.1 Signal Transmitted

In SCMA, each user has a specific codebook, which contains constellation points of dimensions: $\chi_j = \{x_{j1}, x_{j1}, \dots, x_{jM}\}$, among them, the steps of constellation mapping and sparse coding are combined, and each user sends the transmitted bit data signal through codebook coding mapping to obtain a 4-dimensional complex code words, in which the codebook is from literature [17], and then performs parallel serial conversion on the code words combined by 6 users, The obtained serial complex signal is modulated by ACO-OFDM to obtain a serial non negative real signal, and then the serial non negative real signal is converted into a parallel four-way non negative real signal, which is carried on the four primary color LEDs of R, G, B and Y. the signal is transmitted through four optical

carriers. The number of subcarriers transmitted by OFDM is n , so the expression of the transmission signal carried by each subcarrier in the frequency domain is [16]:

$$X_n = \sum_{j=1}^{J\Sigma} \text{diag} \left(\sqrt{P_j} \right) X_{n,j} \quad (1)$$

Here, n represents the n th subcarrier, ($n = 1, \dots, N$), and P_j represents the signal power of the j th user. The transmission signal after ACO-OFDM modulation is [6]:

$$X_{t_ACO-OFDM} = [0, X_1, 0, X_2, \dots, 0, X_N, 0, X_N^*, 0, X_{N-1}^*, \dots, 0, X_1^*]^T \quad (2)$$

The signal sent through the four basic color light carrier is:

$$x_T = x_R + x_G + x_B + x_Y \quad (3)$$

2.2 Channel Model

As shown in Figs. 2 and 3, the LED lamp carrying user information is fixed somewhere on the ceiling. Each receiving user uses a photo detector (PD) to receive the signal light. The separation between the plane of PD receiver and the LED light is h . Here we assume that the radius of the receiver is r . After the user information is sent by the LED light, the optical signal received by the receiving end can be expressed as [13]:

$$y = hx + n \quad (4)$$

Here, h denotes the channel gain of the whole downlink, x represents the signal sent by the LED, and n represents the additive Gaussian white noise (AWGN), which obeys the $(0, \sigma^2)$ normal distribution. The channel gain here h is the sum of direct channel (LoS) and indirect channel (NLoS). Nevertheless, in the case of indoor visible light communication scenarios, the signal of NLoS is very small compared with LoS. Based on this, the expression of visible light channel gain here is as follows:

$$h = \frac{(m+1) n_c^2 Ar x T_s}{2\pi \sin(\Psi)^2} \cos(\phi)^m \frac{\cos(\psi)}{d^2} \text{rect} \left(\frac{\psi}{\Psi} \right) \quad (5)$$

Here m represents the Lambert radiation order, $m = \frac{-\log(2)}{\log(\cos(\phi_{1/2}))}$, $\phi_{1/2}$ represents the half power angle emitted from the LED, Arx denotes the PD receiving area, n_c represents the refractive index of receiving lens, Ψ is the PD detector field of view, d is the direct link separation between the receiver and the LED, ψ stands for the angle of incident of the light, $\text{rect} \left(\frac{\psi}{\Psi} \right)$ is the rectangular function among $[\psi, \Psi]$, T_s is the gain coefficient of the filter, as illustrated in Fig. 1, $\cos(\phi) = \frac{H}{d}$, $d = \sqrt{r^2 + H^2}$, so

$$h = \frac{(m+1) n_c^2 Ar x T_s}{2\pi \sin(\Psi)^2} H^m \frac{\cos(\psi)}{(r^2 + H^2)^{\frac{(m+2)}{2}}} \text{rect} \left(\frac{\psi}{\Psi} \right) \quad (6)$$

2.3 Signal Receiver

The driver color mixed signal transmitted through the visible light channel is received by PD after passing through the filter. After parallel serial conversion, the signal received by the four parallel PD is demodulated by ACO-OFDM, and the expression of the received signal is [13]

$$y = \rho\gamma \sum_{j=1}^J \text{diag} \left(h\sqrt{P_j} \right) x_j + n \quad (7)$$

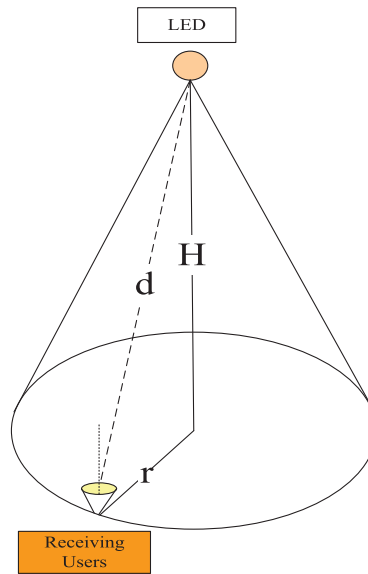


Figure 2: Indoor visible light channel model

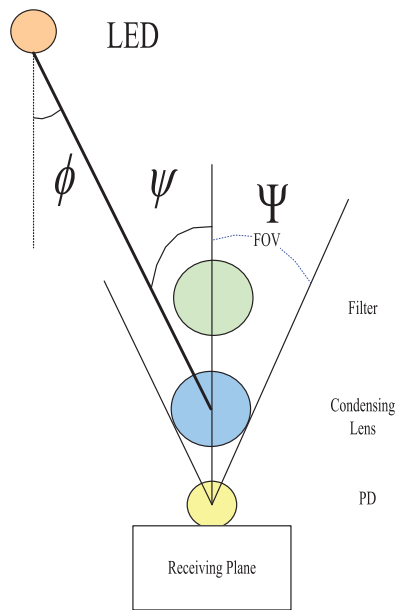


Figure 3: LED transmitting and receiving model

Here, γ is the responsiveness of PD detector and ρ is the photoelectric conversion factor; n represents additive Gaussian white noise, $n \sim \mathcal{CN}(0, \sigma_n^2 I)$

After channel equalization of the received signal, the received signal after equalization at this time is

$$\tilde{y} = \sum_{j=1}^J \text{diag}(\sqrt{P_j}) x_j + \frac{n}{\rho\gamma h} \tag{8}$$

Here, because we only consider the case of direct channel, there is no influence of multipath effect, so the value of $\rho\gamma h$ is a fixed value, which is to say, $\frac{n}{\rho\gamma h}$ is still subject to white noise of Gaussian distribution, let $\tilde{n} = \frac{n}{\rho\gamma h}$, then $\tilde{n} \sim \mathcal{CN}(0, \sigma_{\tilde{n}}^2 I)$

2.4 Signal to Noise Ratio Analysis

Optical power received by the receiver [18,19]

$$Pr = hPt \quad (9)$$

$$Pt = PLED \quad (10)$$

$$SNRr = \frac{(\rho\gamma Pr)^2}{\sigma_{total}^2} \quad (11)$$

$$SNRTX = \frac{(\rho Pt)^2}{\sigma_{total}^2} \quad (12)$$

$SNRr$ Is received signal-to-noise ratio and $SNRTX$ is transmitted signal-to-noise ratio; Here, γ represents the responsiveness of PD detector and ρ represents the photoelectric conversion factor;

$$\sigma^2 total = \sigma^2 shot + \sigma^2 thermal + \sigma^2 am \quad (13)$$

$\sigma^2 shot$ represents the variance of shot noise,

$$\sigma^2 shot = 2q\gamma PrB + 2q\gamma PbgI2B \quad (14)$$

Here, q represents the charge constant, B is the noise bandwidth, Pbg is the ambient noise power, and $I2$ is the noise bandwidth factor of square wave pulse forming at the sending end [20]

$$\sigma^2 thermal = \frac{8\pi kTA}{G} \eta AI2B^2 + \frac{16\pi^2 kTA\Gamma}{g_m} \eta^2 A^2 I_3 B^3 \quad (15)$$

Here TA denotes the absolute temperature of ambient environment, G is the gain of open-loop voltage, η is the unit area capacitance of the PD detector, Γ is the channel noise coefficient of FET (field effect transistor), g_m is the trans conductance of FET field effect transistor, I_3 is the noise bandwidth factor formed by the completely boosted cosine equalization pulse, and k is the Boltzmann constant [21,22]. $\sigma^2 am$ represents the noise bandwidth of the amplification circuit at the receiver

$$\sigma^2 am = i_{am}^2 B_a \quad (16)$$

i_{am} represents the noise intensity of the amplifier and B_a is the response bandwidth of the amplifier;

Add signal to noise ratio of ambient noise

$$SNR'TX = \frac{Pt}{\sigma_{total}^2 + \sigma_{bg}^2} \quad (17)$$

$$\text{Then } SNR'TX = \frac{Pt/\sigma_{total}^2}{\sigma_{total}^2/\sigma_{total}^2 + \sigma_{bg}^2/\sigma_{total}^2} = \frac{SNR_{TX}}{1 + \sigma_{bg}^2 SNR_{TX}/Pt}$$

2.5 SCMA Decoding and Bit Error Rate Performance Analysis

Here, we use MPA (message passing algorithm) as the decoding method. According to the theoretical derivation in the literature, in the AWGN channel, the received signal expression and theoretical bit error rate formula of SCMA system based on the codebook of star QAM constellation points [16] is

$$y_{AWGN} = \sum_{j=1}^J \text{diag}(\sqrt{P_j}) x_j + n \quad (18)$$

$$p_{b-AWGN} = \frac{1}{2n\pi} \int_0^{2\pi - \frac{16\pi}{11M-12}} \exp \left[-\frac{n \frac{E_b}{N_0} \sin^2 \frac{8\pi}{11M-12}}{1 - \cos \frac{8\pi}{11M-12} \cos \left(\frac{8\pi}{11M-12} + \phi \right)} \right] d\phi \quad (19)$$

Comparing the received signals \tilde{y} in the visible light channel, we can find that the types of \tilde{y} and y_{AWGN} are consistent, so the theoretical average bit error rate in the visible light channel can be directly used in the theoretical bit error rate formula in the AWGN channel. In this way, we obtain the theoretical BER formula for 6 users and 4 resource blocks in the visible light channel as

$$p_{b-VLC} = \frac{1}{2n\pi} \int_0^{2\pi - \frac{16\pi}{11M-12}} \exp \left[-\frac{n \frac{E_b}{N_0} \sin^2 \frac{8\pi}{11M-12}}{1 - \cos \frac{8\pi}{11M-12} \cos \left(\frac{8\pi}{11M-12} + \phi \right)} \right] d\phi \quad (20)$$

Here, we use the complex codebook of 4-dimensional columns, where, $M = 2^n$, $M = 2^n \{n = 1, 2, 3, \dots\}$

$$\frac{E_b}{N_0} = SNR - 10 \log_{10}(3) \text{ dB} \quad (21)$$

3 Simulation Results and Analysis

3.1 Parameters

The Channel parameters and SNR parameters are shown in [Tables 1](#) and [2](#), respectively.

Table 1: Channel parameters

Parameter	Value
Height of LED from PD receiving plane H	2.15
PD receiving area A_{rx}	1 cm ²
PD responsiveness γ	0.54 A/W
PD field angle Ψ	60°
LED half power angle $\phi_{1/2}$	60°
Refractive index of condensing lens nc	1.5
Incident angle of LED signal light to PD ψ	60°

3.2 SNR Parameters

Table 2: SNR parameters

Parameter	Value
$PLED$	0.1 W
LED photoelectric conversion factor ρ	0.7 w/A
Noise bandwidth B	50 MHz
Ambient noise power P_{bg}	0.19272 mW
Noise bandwidth factor I_2	0.562
Noise bandwidth factor I_3	0.868
Absolute temperature of surrounding environment TA	300 k
Open loop voltage gain G	10
PD capacitance per unit area η	$1.12\mu\text{F}/\text{m}^2$
FET channel noise coefficient Γ	1.5
FET trans conductance g_m	30 mS
Amplifier noise intensity i_{am}	$5\text{ pA}/\sqrt{\text{Hz}}$
Response bandwidth of amplifier B_a	50 MHz

3.3 Simulation Results and Analysis

From the Fig. 4, we can see that the simulation results of $m = 4, 8, 16$ of codebook are roughly consistent with the theoretical analysis results without adding environmental noise, and we can see that $m = 8$ is that the simulation results are basically consistent with the theoretical analysis, which shows that the codebook we use is indeed feasible in visible light communication, and we have found the aco-ofd of SCMA using this codebook.

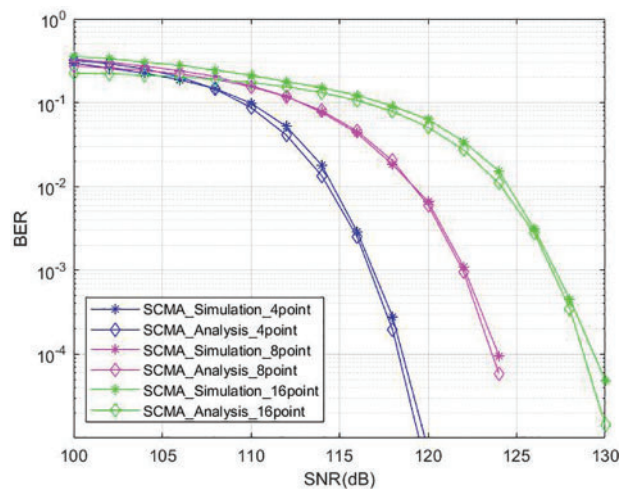


Figure 4: $m = 4, 8, 16$; theoretical and simulated bit error rate curve at 4, 8, 16 (without environmental noise)

Figs. 5–7 are the comparison of the theoretical bit error rate and the simulation bit error rate with and without environmental noise at different m values, that is, under the constellation points of the codebook mapping that are not used. From the comparison results, with low transmission SNR, the theoretical BER and the simulation bit error rate with and without environmental noise are consistent. With the continuous increase of the transmission signal-to-noise ratio, The bit error rate with ambient noise is significantly lower than that without ambient noise. And we can see from the signal-to-noise ratio formula added with environmental noise that when the transmission signal-to-noise ratio increases to a certain extent, its simulation and theoretical bit error rate will tend to be stable, which also shows that we cannot only increase the SNR to decrease the system’s error rate, but also must find other ways to improve the anti noise performance of the system.

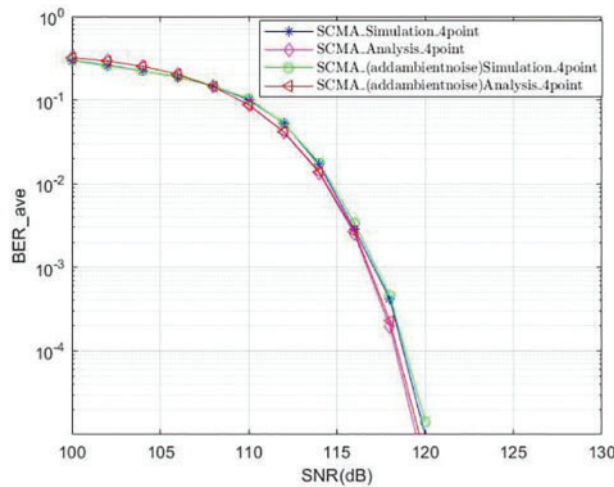


Figure 5: m = 4 comparison diagram of adding environmental noise and not adding environmental noise

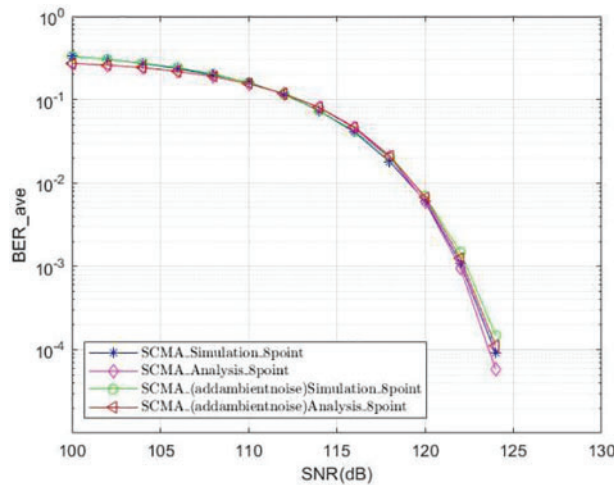


Figure 6: m = 8 comparison diagram of adding environmental noise and not adding environmental noise

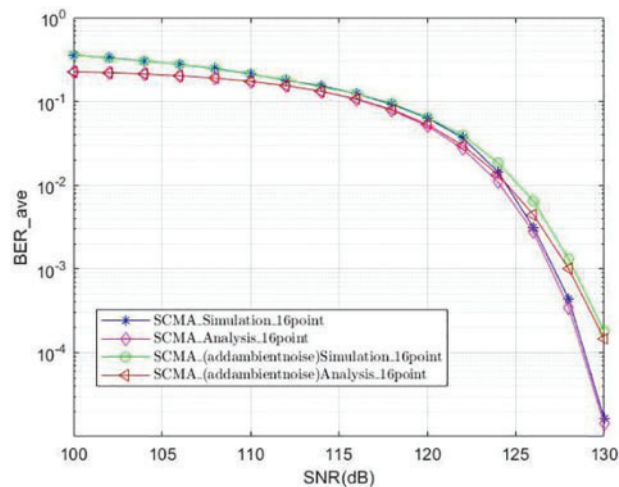


Figure 7: $m = 16$ comparison diagram of adding environmental noise and not adding environmental noise

4 Conclusion

In this paper, we propose an QACO-OFDM visible light communication system based on SCMA. In this system, we consider the sparse codebook based on Star QAM constellation point mapping to map the bit information flow of multiple users, and its overload rate is $j/k = 150\%$. ACO-OFDM technology can be used to achieve high-speed visible light communication. The simulation results show that the simulation results are basically consistent with the theoretical analysis results after considering the actual system noise. The research of this paper provides a solid theoretical basis for the application of NOMA technology to the field of next-generation mobile communication.

Funding Statement: The work is not supported by any funding.

Availability of Data and Materials: The raw data supporting the conclusions of this article will be made available by the authors, without undue reservation.

Conflicts of Interest: The authors declare that they have no conflicts of interest to report regarding the present study.

References

- [1] L. Eduardo Mendes Matheus, A. Borges Vieira, L. F. M. Vieira, M. A. M. Vieira and O. Gnawali, "Visible light communication: Concepts, applications and challenges," *IEEE Commun. Surveys Tuts.*, vol. 21, no. 4, pp. 3204–3237, 4th Quart., 2019.
- [2] S. Ma, Q. Liu and P. C. -Y. Sheu, "Foglight: Visible light-enabled indoor localization system for low-power IoT devices," *IEEE Internet Things J.*, vol. 5, no. 1, pp. 175–185, 2018.
- [3] P. H. Pathak, X. Feng, P. Hu and P. Mohapatra, "Visible light communication, networking, and sensing: A survey, potential and challenges," *IEEE Commun. Surveys Tuts.*, vol. 17, no. 4, pp. 2047–2077, 2015.
- [4] S. Al-Ahmadi, O. Maraqa, M. Uysal and S. M. Sait, "Multi-user visible light communications: State-of-the-art and future directions," *IEEE Access*, vol. 6, pp. 70555–70571, 2018.
- [5] C. Chen, W. -D. Zhong, H. Yang and P. Du, "On the performance of MIMO-NOMA-based visible light communication systems," *IEEE Photon. Technol. Lett.*, vol. 30, no. 4, pp. 307–310, 2018.

- [6] J. Yanling, "Research on optical wireless communication system based on ACO-OFDM," *Ph.D. Dissertation*, Harbin Engineering University, China, 2016.
- [7] Z. Ma, Z. Zhang, Z. Ding, P. Fan and H. Li, "Key techniques for 5G wireless communications: Network architecture, physical layer, and MAC layer perspectives," *Sci. China Inf. Sci.*, vol. 58, no. 4, pp. 1–20, 2015.
- [8] Y. Saito, Y. Kishiyama, A. Benjebbour, T. Nakamura and A. Li, "Non-orthogonal multiple access (NOMA) for cellular future radio access," in *Proc. IEEE VTC-Spring*, Dresden, Germany, pp. 1–5, 2013.
- [9] H. Nikopour and H. Baligh, "Sparse code multiple access," in *Proc. IEEE PIMRC*, London, U.K., pp. 332–336, 2013.
- [10] J. van de Beek and B. M. Popovic, "Multiple access with lowdensity signatures," in *Proc. IEEE GLOBECOM*, Honolulu, HI, USA, pp. 1–6, 2009.
- [11] R. Hoshyar, F. P. Wathan and R. Tafazolli, "Novel low-density signature for synchronous CDMA systems over AWGN channel," *IEEE Trans. Signal Process.*, vol. 56, no. 4, pp. 1616–1626, 2008.
- [12] R. Mitra, S. Sharma, G. Kaddoum and V. Bhatia, "Color-domain SCMA NOMA for visible light communication," *IEEE Commun. Lett.*, early access, vol. 25, no. 1, pp. 200–204, 2020. <https://doi.org/10.1109/LCOMM.2020.3023058>
- [13] B. Lin, X. Tang and Z. Ghassemlooy, "A power domain sparse code multiple access scheme for visible light communications," *IEEE Wireless Commun. Lett.*, vol. 9, no. 1, pp. 61–64, 2020.
- [14] B. Lin, X. Tang, Z. Zhou, C. Lin and Z. Ghassemlooy, "Experimental demonstration of SCMA for visible light communications," *Opt. Commun.*, vol. 419, pp. 36–40, 2018.
- [15] J. An and W. -Y. Chung, "Single-LED multichannel optical transmission with SCMA for long range health information monitoring," *J. Lightw. Technol.*, vol. 36, no. 23, pp. 5470–5480, 2018.
- [16] L. Yu, P. Fan, X. Lei and T. Mathiopoulos, "BER analysis of SCMA systems with codebooks based on star-QAM signaling constellations," *IEEE Commun. Lett.*, vol. 21, no. 9, pp. 1925–1928, 2017.
- [17] L. Yu, X. Lei, P. Fan and D. Chen, "An optimized design of SCMA codebook based on starQAM signaling constellations," in *Proc. IEEE WCSP*, Nanjing, China, pp. 1–5, 2015.
- [18] M. A. Arfaoui, M. D. Soltani, I. Tavakkolnia, A. Ghrayeb, C. Assi *et al.*, "SNR statistics for indoor VLC mobile users with random orientation," in *Proc. IEEE ICC*, Shanghai, China, pp. 1–6, 2019.
- [19] H. Lu, Z. Su and B. Yuan, "SNR and optical power distribution in an indoor visible light communication system," in *Proc. of the 7th Int. Congress on Image and Signal Processing*, Dalian, pp. 1063–1067, 2014.
- [20] S. -J. Lee and S. -Y. Jung. "A SNR analysis of the visible light channel environment for visible light communication," in *2012 18th Asia Pacific Conf. on Communications (APCC)*, Jeju Island, IEEE, 2012.
- [21] L. Yu, P. Fan, D. Cai and Z. Ma, "Design and analysis of SCMA codebook based on star-QAM signaling constellations," *IEEE Trans. Vehic. Tech.*, vol. 67, no. 11, pp. 10543–10553, 2018.
- [22] L. Yu, Z. Liu, M. Wen, D. Cai, S. Dang *et al.*, "Sparse code multiple access for 6G wireless communication networks: Recent advances and future directions," *IEEE Communications Standards Magazine*, vol. 5, no. 2, pp. 92–99, 2021.